Published in final edited form as:

IEEE Trans Electromagn Compat. 2006 June 5; 48(2): 397–407. doi:10.1109/TEMC.2006.873870.

Comparisons of Computed Mobile Phone Induced SAR in the SAM Phantom to That in Anatomically Correct Models of the Human Head

Brian B. Beard,
Center for Devices and Radiological Health, Food and Drug Administration, Rockville, MD 20850 USA

Wolfgang Kainz [Member, IEEE],
Center for Devices and Radiological Health, Food and Drug Administration, Rockville, MD 20850 USA

Teruo Onishi [Member, IEEE],
Wireless Laboratories, NTT DoCoMo, Inc. NTT DoCoMo R&D Center, Kanagawa, 239-8536, Japan

Takahiro Iyama,
Wireless Laboratories, NTT DoCoMo, Inc. NTT DoCoMo R&D Center, Kanagawa, 239-8536, Japan

Soichi Watanabe [Member, IEEE],
National Institute of Information and Communications Technology (NICT) Tokyo 184-8795, Japan

Osamu Fujiwara [Member, IEEE],
Graduate School of Engineering, Nagoya Institute of Technology, Nagoya 466-8555, Japan

Jianqing Wang,
Graduate School of Engineering, Nagoya Institute of Technology, Nagoya 466-8555, Japan

Giorgi Bit-Babik [Member, IEEE],
Motorola Florida Research Laboratories, Corporate EME Research Laboratory, Fort Lauderdale, FL 33322 USA

Antonio Faraone [Senior Member, IEEE],
Motorola Florida Research Laboratories, Corporate EME Research Laboratory, Fort Lauderdale, FL 33322 USA

Joe Wiart [Senior Member, IEEE],
France Telecom FTRD/RESA/FACE/IOP 92794 Issy les Moulineaux, France

Andreas Christ,
IT'IS–The Foundation for Research on Information Technologies in Society, Zurich, Switzerland

---

The opinions and conclusions stated in this article are those of the authors and do not represent the official position of the United States Food and Drug Administration. The mention of commercial products, their sources, or their use in connection with material reported herein is not to be construed as either an actual or implied endorsement of such products by the United States Food and Drug Administration.

Niels Kuster [Member, IEEE],
IT'IS–The Foundation for Research on Information Technologies in Society, Zurich, Switzerland

Ae-Kyoung Lee,
Electronics and Telecommunications Research Institute (ETRI), Daejeon, 305-350 Korea

Hugo Kroeze,
Department of Radiotherapy, University of Utrecht, 3508 GA Utrecht, The Netherlands

Martin Siegbahn,
Ericsson Radio Systems AB S-164 80 Stockholm, Sweden

Jafar Keshvari,
Radio Technologies Laboratory, Nokia Research Center, 00180 Helsinki, Finland

Houman Abrishamkar,
Department of Electrical and Computer Engineering, University of Victoria, Victoria, BC V8W 3P6 Canada

Winfried Simon,
IMST GmbH, Antennas and EM Modelling 47475 Kamp-Lintfort Germany

Dirk Manteuffel, and
IMST GmbH, Antennas and EM Modelling 47475 Kamp-Lintfort Germany

Neviana Nikoloski
IT'IS–The Foundation for Research on Information Technologies in Society, Zurich, Switzerland

Abstract

The specific absorption rates (SAR) determined computationally in the specific anthropomorphic mannequin (SAM) and anatomically correct models of the human head when exposed to a mobile phone model are compared as part of a study organized by IEEE Standards Coordinating Committee 34, SubCommittee 2, and Working Group 2, and carried out by an international task force comprising 14 government, academic, and industrial research institutions. The detailed study protocol defined the computational head and mobile phone models. The participants used different finite-difference time-domain software and independently positioned the mobile phone and head models in accordance with the protocol. The results show that when the pinna SAR is calculated separately from the head SAR, SAM produced a higher SAR in the head than the anatomically correct head models. Also the larger (adult) head produced a statistically significant higher peak SAR for both the 1- and 10-g averages than did the smaller (child) head for all conditions of frequency and position.

Index Terms

FDTD methods; IEEE standards; phantom; simulation; software standards; specific absorption rate (SAR); specific anthropomorphic mannequin (SAM)

I. Introduction

A. Background

Mobile phone safety and the enforcement of applicable exposure standards are frequent topics in the popular media, and regulatory agencies are striving to insure that compliance testing is accurate. IEEE Standard 1528 [1] and IEC 62209-1 [2] specify protocols and procedures for the measurement of the peak spatial-average specific absorption rate (SAR) induced inside a simplified model of the head of the users of handheld radio transceivers (mobile phones). Both IEEE and IEC standards provide regulatory agencies with international consensus standards as a reference for accurate compliance testing. The simplified physical model (phantom) of the human head specified in IEEE 1528 and IEC 62209-1 is the specific anthropomorphic mannequin (SAM). SAM has also been adopted by the European Committee for Electrotechnical Standardization (CENELEC) [3], the Association of Radio Industries and Businesses in Japan [4], and the Federal Communications Commission in the USA [5].

SAM was developed by the IEEE Standards Coordinating Committee 34, Subcommittee 2, Working Group 1 (SCC34/SC2/WG1) as a lossless plastic shell and an ear spacer. Because current technology does not allow reliable measurement of the SAR in small complex structures, such as a simulated pinna, while maintaining the anatomical structure's integrity, SCC34/SC2/WG1 chose to use a thin lossless ear spacer on SAM to maximize the energy reaching the head and minimize the measurement uncertainty. The need to maintain the essential features of the ear anatomy in order to correctly estimate the SAR in the head was pointed out in [6], where it was also shown that a lossless spacer would not produce SAR underestimation in the head. The SAM shell is filled with a homogeneous fluid having the electrical properties of head tissue at the test frequency. The dielectric properties of the fluid were based on calculations to give conservative spatial-average SAR values averaged over 1 and 10 g for the test frequencies [7].

A primary design goal for SAM was that "SAM shall produce a conservative SAR for a significant majority of persons during normal use of wireless handsets" [1]. To determine the extent to which SAM is truly conservative, various investigators have used computational radio frequency (RF) dosimetry to compare the SAR in SAM to that in anatomically correct models of the human head. These anatomically correct head models are commonly derived from MRI scans. Some investigators found that SAM underestimates SAR in adults and children by a factor of 2 or more [8], [9]. Other investigators found that SAM overestimates SAR in both adults and children [10], [11]. These contradictory findings may lead to confusion in the lay public and raise the concern of regulatory agencies. Further, they call into question the validity of computational RF dosimetry and the conservative nature of SAM. Other reports have presented mixed results [12]–[26], further adding to the confusion.

The SCC34/SC2/WG2, whose purpose is to develop computational techniques for determining the SAR in the human body due to wireless communications devices [27], set out to analyze and resolve the causes for the reported discrepancies. A close examination of the literature revealed several procedural and reporting issues that could account for the discrepancies [28].

B. Potential Causes of Discrepancies

Inclusion versus exclusion of the pinna from the 1- or 10-g SAR averaging volumes is the first and most significant cause. Some investigators [8], [9] treated the pinna in accordance with ICNIRP Guidelines [29] that apply the same peak spatial SAR limits for the pinna and the head. Because the pinna is usually the tissue closest to the feed point of a mobile phone antenna, the highest point SAR values are usually found in the pinna; consequently, averaging volumes that include pinna tissue produce higher SAR.

Other investigators [10], [11] treated the pinna in accordance with, what was then a draft but is now published, IEEE Standard C95.1b-2004 [30], which applies the peak spatial SAR limits for the extremities to the pinnae. The SAR limit for extremities and pinnae is 4 W/kg per 10-g mass rather than the 1.6 W/kg per 1 g for the body and head. Because of the different peak SAR limits and averaging masses, IEEE Standard C95.3-2002 spec-ifies methods for calculating the peak spatial SAR in the head and pinna [31]. These investigators excluded pinna tissue from their head tissue SAR averaging. However, within this group the definition of head tissue versus pinna tissue was inconsistent and often not described at all. When comparing published results, it was often difficult or impossible to determine whether the head tissue SAR values were based on averaging volumes that included or excluded the pinna. In fact, some papers make no mention of how the pinna was treated.

The second cause of discrepancies is the lack of a common database of anatomically correct models. Investigators have used several different models but the only ones that can be compared across all the published results are the SAM and the Visible Human. The anatomical data for the Visible Man originated at the U.S. National Library of Medicine and many research labs, such as Brooks Air Force Base, and individual researchers converted it into finite-difference time-domain (FDTD) models. This means that the only repeatable comparison that can be made is between the SAM and the Visible Human. It seems obvious that one can neither prove nor disprove that the SAM produces a conservative SAR for a significant majority of persons during normal use of wireless handsets, when there is only one anatomically correct model available for comparison.

Modeling of the electromagnetic source may have also contributed to the reported discrepancies. A dipole was the only model used in more than one study [6], [14], [32], [33]. Simulation models of mobile phones have varied in size, shape, antenna type, antenna length, and sophistication.

The third cause of discrepancies is inconsistent positioning of the mobile phone model relative to the head model. Simulated SAR in near-field exposure conditions is mainly a function of the source geometry, the RF current density distribution on the source, and its geometric separation from the lossy head tissue [1]. When the separation distance is small, a 1- or 2-mm change can significantly alter the SAR obtained for a specific mobile phone and head model [33], [34]. The computer aided design (CAD) files defining SAM show specific reference points and lines to be used to position mobile phones for the two compliance test positions specified in [1] and [2]. These are the *Cheek* position shown in Fig. 1 and the *Tilt* position shown in Fig. 2. The reference points are not available on anatomically correct models of the head. These reference points can be defined with respect to anatomical

features, but the interpretation of these anatomical features can vary between investigators. Consequently, even if two investigators use the same mobile phone and head models, there is no assurance that the positioning of the mobile phone relative to the head model is the same.

Differences in the FDTD software are the fourth potential cause of discrepancies. The basic FDTD algorithm requires a voxelized model. Usual practice is to align the mobile phone antenna with the FDTD voxel grid to avoid the staircase effect as much as possible. The head model is then rotated to the correct position relative to the mobile phone. After rotation, the model must be remeshed to align the voxels with the FDTD grid. Artifacts have been noted in some models after this meshing [24]. These artifacts include distortion of smooth boundaries between tissue types, creation of isolated tissue regions in other tissue types, and creation of empty voxels (air) along a tissue boundary. Any of these artifacts, if not manually corrected, can have a significant effect on the local SAR.

Another potential cause of discrepancies of results is the manner in which the SAR is normalized for reporting. Some investigators have chosen to normalize their results to net input power, while others have used feed-point current. When the mobile phone model is placed next to the SAM or anatomically correct model, it changes the mobile phone's antenna feed-point impedance. The antenna feed-point impedance (Z), feed-point current (I), and net input power (P_{net}) are related by

$$P_{\text{net}}=\frac{1}{2}|\hat{I}|^2\text{Re}\{Z\} \quad (1)$$

Several studies [14], [15] have shown that the feed-point impedance depends on the head model, the size of the head next to the mobile phone, the position of the mobile phone, and the mobile phone model itself. Because different head models or test conditions would not produce the same feed-point impedance, the SAR normalized to net input power or feed-point current may exhibit distinct trends. It should be noted that the results normalized to net power are more applicable to practical cases than results normalized to feed-point current due to internal power control or limitation mechanism in wireless products.

Finally, a potential contributor to the observed discrepancies is the difference in SAR averaging algorithms. Some papers lack a detailed description of the averaging methods, and in many cases there are different approaches employed, especially in the way the averaging volume is constructed in the vicinity of tissue-air interfaces where the peak SAR values are usually observed. This may further contribute to discrepancies of the reported results [25].

C. Large Scale Inter-Comparison Study

To address the above problems, the *Protocol for the Computational Comparison of the SAM Phantom to Anatomically Correct Models of the Human Head* was developed by the SCC34/SC2/WG2. The protocol was designed to control known sources of variability so that the conservative nature of SAM could be inferred using FDTD. The protocol was defined in 2003 and each institution reported its results in 2004. The collective data were analyzed on

behalf of the SCC34/SC2/WG2, and a final report, including the collective data set, was issued in May 2004.

This paper, reporting the study outcome, is organized as follows. In Section II, a detailed explanation of the study protocol is presented. In Section III, the collective analysis of the results reported by the participating institutions is described. A discussion on the significance and implications of the results and some final conclusions are presented in Sections IV and V, respectively.

II. Materials and Methods

Each participating institution was provided with the FDTD database for three head models and a generic mobile phone (Fig. 3). The three head models were SAM and two anatomically correct models: the Visible Human (Fig. 4) and a 7-year-old Japanese male [15] (Fig. 5). For the two anatomically correct models, the tissue names and properties were made consistent with the definitions found on the Italian National Research Council, Institute for Applied Physics Web site [35]. The generic mobile phone is formed by a monopole antenna and a chassis, with the excitation point at the base of the antenna. The antenna length is 71 mm for 835 MHz and 36 mm for 1900 MHz, and its square cross section has 1-mm edge. The monopole is coated with a 1-mm thick plastic having dielectric properties $\varepsilon_r = 2.5$ and $\sigma = 0.005$ S/m. The chassis comprises a printed circuit board having lateral dimensions of 40 × 100 mm and thickness of 1 mm, symmetrically embedded in a solid plastic case with dielectric properties $\varepsilon_r = 4$ and $\sigma = 0.04$ S/m, lateral dimensions 42 × 102 mm, and thickness 21 mm. The antenna is mounted along the chassis centerline so as to avoid differences between right- and left-side head exposure. The antenna is a thick-wire model whose excitation is a 50-Ω sinusoidal voltage source at the gap between the antenna and printed circuit board. The generic mobile phone used in this study was designed to be a simple and easily constructed model. It approximates the gross physical and emission characteristics of a typical mobile phone but was not designed for strict compliance with international SAR limits. No hand model was included.

The dielectric properties of the head tissue used in the SAM model are those defined in [1] and [2], while those of its shell and the ear spacer were defined as follows: $\varepsilon_r = 5$ and $\sigma = 0.0016$ S/m. Particular care was used to define the conditions in any FDTD grid that would indicate contact between materials, as this particular aspect, closely related to the phone positioning against the head, was deemed critical.

The protocol called for each participant to run 12 simulations to fill an experiment matrix comprising the three head models, two frequencies (835 and 1900 MHz), and two phone positions (*cheek* and *tilt*). Because of the symmetrical antenna location with respect to the phone chassis, simulations were performed with the phone only on the right hand side of the head.

Participants had to report the peak spatial SAR for 1- and 10-g averaging volumes (computed in accordance with IEEE C95.3-2002 [31] Annex E) that included pinna tissue only, head tissue only, and all (pinna and head) tissues. All results were normalized to both

net input power and feed-point current. The pinna of the anatomical models was predefined in the models used by the participants. The voxels comprising the pinna in the provided anatomical models were flagged in accordance with the IEEE Standard 1528 definition of the pinna, and the choice of each flagged voxel was confirmed by an Ear-Nose-Throat surgeon. The flagging of the pinna voxels did not alter the electrical properties of the anatomic tissue type; skin, cartilage, etc. The reference points, which are necessary for positioning the mobile phone relative to the anatomically correct models, were also defined in the FDTD data set defining each anatomical model.

To aid comparison of results from all the participants, a common coordinate system was defined with origin at the acoustic output of the mobile phone (see Fig. 6). A common framework to define the 15° rotation required to simulate the *tilt* position was established as well.

The protocol, as described, is an exhaustive examination of six independent variables:

1. frequency (835, 1900 MHz);
2. position (*Cheek, Tilt*);
3. model (7-year child, Adult, SAM);
4. tissues considered in the SAR averaging (all, head only, pinna only);
5. SAR averaging volume (1 and 10 g) and averaging method (IEEE Std C95.3-2002);
6. SAR normalization versus net emitted power (1 W) and feed-point current (200 mA).

Thus, a total of 144 unique cases would be defined. However, because SAM has a lossless pinna, the pinna only and all tissue cases are not applicable to the SAM. This reduces the total number of cases requiring SAR averaging to 112.

Participants also reported a number of other results including positioning data, mobile phone impedances in free space, and radiated versus absorbed power.

III. Results

Fourteen institutions participated in the study. Two of the participants provided a second set of results, computed with different FDTD software, for a total of 16 data sets. The results presented herein are kept anonymous.

Of the 16 data sets, eight were computed using unique software, 3 were computed using XFDTD (Remcom, Inc.), and five were computed using SEMCAD (Schmid & Partner Engineering AG). A mixed linear model analysis of variance (ANOVA) was performed across the three types of software: XFDTD, SEMCAD, and other. The results showed there was no significant difference ($p > 0.07$) in results by software type.

Tables I–IV show the mean and standard deviation of the SAR results reported by the participants. As a validation, one of the participants constructed physical representations of

the generic mobile phones at 835 and 1900 MHz [36]. The physical generic mobile phone models were used as the RF source for a limited number of SAR measurements with an actual SAM phantom. The measurement results and the corresponding computational averages are shown in Table V and plotted in Fig. 7.

Tables VI and VII show the statistics for reported distance between the generic mobile phone feed point and the nearest tissue voxel for *cheek* and *tilt* positions, respectively.

The SAR data for the anatomical models was normalized by the SAR for SAM under the same conditions. A mixed linear model ANOVA was performed, with Group as the random effect and with Tissue, Averaging volume, Frequency, Position, Model, and Normalization as fixed effects. Initial results suggested stratification over the three tissue types (all, head only, and pinna only) and also showed that the difference in normalization (1 W or 200 mA) is not statistically significant ($p > 0.06$). Final results showed that the average SAM normalized SAR for the adult model is statistically significantly greater than the average SAM normalized SAR for the 7-year-child model, for each of the three tissue types ($p < 0.02$).

IV. Discussion

Because the SAM phantom is accepted in IEEE and IEC standards for compliance testing, it is convenient to normalize the SAR for the anatomic models to the SAR from SAM for the same conditions. Table VIII shows the normalized mean values and standard deviations of SAR when only head tissue is used for the SAR averaging volume. This table shows the average head only SAR for the anatomic models is consistently less than that for the SAM for all simulated conditions of frequency, position, SAR averaging volume, and normalization. This indicates that if the peak spatial SAR from compliance tests using SAM with a particular mobile phone meets the SAR limit for head tissue, then the exposure of a human head to that particular mobile phone would be below the limit.

Because current SAR test methods do not allow measurements in the pinna, SAM has a lossless ear spacer instead of the pinna. In this study, however, it was possible to compute the SAR in the pinna of the anatomic models using specific SAR averaging techniques. Table IX shows the means and standard deviations of pinna only SAR normalized to the mean SAM SAR for the same exposure conditions. This table shows that the average pinna only SAR for the anatomic models can exceed the SAR in the head for SAM. The highest pinna SAR seen was 1.44 times (144%) the maximum head SAR in SAM. While IEEE Standard C95.1b-2004 calls for 1.6 W/kg over 1 g in the head and 4 W/kg over 10 g in the pinna, the difference in averaging volumes makes direct comparisons difficult. For the ICNIRP guidelines, having the same SAR limit for head and pinna, no firm conclusion can be drawn because the IEEE SAR averaging technique used in the study did not correspond to the averaging mass specified by ICNIRP. Therefore, more detailed investigations of SAR in the pinna may be needed.

To consider whether head size has a consistent effect on SAR, we compared the SAM normalized results for the 7-year-old child model to the adult model. For head tissue only

(Table VIII), the child model peak-SAR was lower than the adult model's in 13 of 16 averages, for pinna tissue only (Table IX) the child model peak-SAR was lower in 11 of 16 averages, and for all tissue (results not shown), the child model peak-SAR was lower in 10 of 16 averages. ANOVA analysis shows that, for all three tissue types, differences among these results are statistically significant. Generalizing from these data one might infer that larger (adult) heads tend to produce larger SAR.

In spite of the steps taken to reduce the variance of the results among all the participants, for each of the 112 cases presented in Tables I–IV the standard deviation is a significant percentage of the mean. Specifically, for the 56 cases at 835 MHz the average standard deviation is 17% of the mean, for 1900 MHz it is 29%. We suspect much of this variation is due to positioning differences as reflected in Tables VI and VII. In the near-field conditions being simulated a few millimeters, change in distance can result in a significant difference in SAR. Differences in positioning distance would produce the highest SAR variance in pinna tissue which, being adjacent to the mobile phone, would experience the greatest relative change in the distance. Small distance changes would produce less variance in the head tissue than in the pinna tissue. Comparing the pinna tissue only standard deviations from Table IX to the head tissue only standard deviations in Table VIII, we find this to be true.

The cause of the positioning variation is believed to be the differences in human judgment when interpreting the instructions for proper positioning of the mobile phone for simulation or compliance testing. An improved method for mobile phone positioning on anatomical models that could be considered for a future computational compliance standards was recently presented [36].

V. Conclusion

The variance of observed results from computer modeling is comparable to that from experimental measures in phantoms, as it is subject to errors and differences in judgment during positioning.

The unique feature of this study is the large number of simulations from multiple institutions; our conclusions are based on the collective averages of the results presented by the participating institutions. As is true with any experiment, our conclusions are applicable only to the situations studied, generalization to other situations may involve factors that alter the conclusions.

When only head tissue is considered, data show that the SAM produces higher SAR than the anatomically correct models that were considered. This leads us to conclude that the SAM does produce a conservative estimate of SAR in the head and assures compliance with respect to the international exposure guidelines. The larger (adult) head resulted in a statistically higher peak SAR than did the smaller (child) head for all conditions. Peak SAR in the pinna of the anatomically correct models was slightly higher than the head SAR seen in SAM, which indicates that local SAR averaging techniques in this region may need further consideration.

Acknowledgments

IEEE SCC-34/SC-2/WG-2 would like to thank the Mobile Manufacturers Forum for their support of our meetings.

The authors would like to thank Dr. E. Mann of the US FDA, Office of Device Evaluation, for his assistance in defining the pinna in the anatomically correct models; M. Stuchly from the University of Victoria and O. Gandhi and G. Kang from the University of Utah, for contributing data to the study; and H. Bushar of the US FDA, Office of Surveillance and Biometrics, for his assistance with statistical analysis.

References

1. *Recommended Practice for Determining the Peak Spatial-Average Specific Absorption Rate (SAR) in the Human Head from Wireless Communications Devices: Measurement Techniques*, IEEE Standard 1528–2003, 2003.
2. *Human Exposure to Radio Frequency Fields from Hand-Held and Body-Mounted Wireless Communication Devices—Human Models, Instrumentation, and Procedures—Part 1: Procedure to Determine the Specific Absorption Rate (SAR) for Hand-Held Devices Used in Close Proximity to the Ear (Frequency Range of 300 MHz to 3 GHz)*, IEC 62209-1, 2005.
3. *Basic Standard for the Measurement of Specific Absorption Rate Related to Exposure to Electromagnetic Fields from Mobile Phones (300 MHz–3 GHz)*, EN 50361, 2001.
4. *Specific Absorption Rate (SAR) Estimation for Cellular Phone*, ARIB STD-T56, 2002.
5. "*Federal Communications Commission (FCC) Evaluating Compliance with FCC Guidelines for Human Exposure to Radio Frequency Electromagnetic Fields,*" Supplement C to OET Bulletin 65 (Edition 9701), Washington, DC: FCC, 1997 inSupplement C to OET Bulletin 65 (Edition 9701), Washington, DC: FCC, 1997.
6. Kanda M, Balzano Q, Russo P, Faraone A, Bit-Babik G. Effects of ear-connection modeling on the electromagnetic-energy absorption in a human head phantom exposed to a dipole antenna field at 835 MHz. IEEE Trans Electromagn Compat. Feb; 2002 44(1):4–10.
7. Drossos A, Santomaa V, Kuster N. The dependence of electromagnetic energy absorption upon human head tissue composition in the frequency range of 300–3000 MHz. IEEE Trans Microw Theory Tech. Nov; 2000 48(11):1988–1995.
8. Gandhi OP, Kang G. Some present problems and a proposed experimental phantom for SAR compliance testing of cellular telephones at 835 and 1900 MHz. Phys Med Biol. 2002; 47:1501–1518. [PubMed: 12043816]
9. Gandhi OP, Kang G. Inaccuracies of a plastic pinna SAM for SAR testing of cellular telephones against IEEE and ICNIRP safety guidelines. IEEE Trans Microw Theory Tech, pt 2. Aug; 2004 52(8):2004–2012.
10. Kuster, N., Christ, A., Chavannes, N., Nikoloski, N., Frölich, J. Human head phantoms for compliance and communication performance testing of mobile telecommunication equipment at 900 MHz. presented at the 2002 Interim Int. Symp. Antennas Propag; Yokosuka Research Park, Yokosuka, Japan. Nov. 26–28 2002;
11. Christ A, Chavannes N, Nikoloski N, Gerber H, Pokovic K, Kuster N. A numerical and experimental comparison of human head phantoms for compliance testing of mobile telephone equipment. Bioelectromagnetics. 2005; 26:125–137. [PubMed: 15672370]
12. Lee A, Choi H, Lee H, Pack J. Human head size and SAR characteristics for handset exposure. ETRI J. Apr.2002 24:176–179.
13. Dimbylow PJ, Mann SM. SAR calculations in an anatomically realistic model of the head for mobile communications transceivers at 900 MHz and 1.8 GHz. Phys Med Biol. 1994; 39:1537–1553. [PubMed: 15551530]
14. Van de Kamer JB, Lagendijk JJW. Computation of high-resolution SAR distributions in a head due to a radiating dipole antenna representing a hand-held mobile phone. Phys Med Biol. 2002; 47:1827–1835. [PubMed: 12069097]
15. Wang J, Fujiwara O. Comparison and evaluation of electromagnetic absorption characteristics in realistic human head models of adult and children for 900-MHz mobile telephones. IEEE Trans Microw Theory Tech. Mar; 2003 51(3):966–971.

16. Okoiewski M, Stuchly MA. A study of the handset antenna and human interaction. IEEE Trans Microw Theory Tech, pt 2. Oct; 1996 44(10):1855–1864.
17. Hombach V, Meier K, Burkhardt M, Kühn E, Kuster N. The dependence of EM energy absorption on human head modeling at 900 MHz. IEEE Trans Microw Theory Tech, pt 2. Oct; 1996 44(10): 1865–1873.
18. Bernardi P, Cavagnaro M, Pisa S. Evaluation of the SAR distribution in the human head for cellular phones used in a partially closed environment. IEEE Trans Electromagn Compat. Aug; 1996 38(3):357–366.
19. Wiart J, Dale C, Bosisio AV, Le Cornec A. Analysis of the influence of the power control and discontinuous transmission on RF exposure with GSM mobile phones. IEEE Trans Electromagn Compat. Nov; 2000 42(4):376–385.
20. Luebbers, R., Baurle, R. FDTD predictions of electromagnetic field in and near human bodies using visible human project anatomical scans. Proc. IEEE AP-S Int. Symp. and URSI Radio Sci. Meeting; Baltimore, MD. Jul. 21–26, 1996; p. 1806-1809.
21. Martinez-Burdalo M, Martin A, Anguiano M, Villar R. Comparison of FDTD-calculated specific absorption rate in adults and children when using a mobile phone at 900 and 1800 MHz. Phys Med Biol. 2004; 49:345–354. [PubMed: 15083675]
22. Gandhi OP, Lazzi G, Furse CM. Electromagnetic absorption in the human head and neck for mobile telephones at 835 and 1900 MHz. IEEE Trans Microw Theory Tech, part 2. Oct; 1996 44(10):1884–1897.
23. Hadjem, A., Lautru, D., Dale, C., Wong, M., Fouad-Hanna, V., Wiart, J. Comparison of specific absorption rate (SAR) induced in child-sized and adult heads using a dual band mobile phone. Proc. IEEE MTT-S IMS-2004; Jun. 6–11, 2004; p. 1453-1456.
24. Mochizuki S, Watanabe S, Taki M, Yamanaka Y, Shirai H. Size of head phantoms for standard measurements of SAR due to wireless communication devices. Electron Commun Jpn (Part 1: Communications). 2004; 87(4):82–91.
25. Bit-Babik G, Guy AW, Chou CK, Faraone A, Kanda M, Gessner A, Wang J, Fujiwara O. Simulation of exposure and SAR estimation for adult and child heads exposed to RF energy from portable communication devices. Radiat Res. 2005; 163:580–590. [PubMed: 15850420]
26. Lee A, Choi H, Choi J, Pack J. Specific absorption rate values of handsets in cheek position at 835 MHz as a function of scaled specific anthropomorphic mannequin models. ETRI J. Apr.2005 27:227–230.
27. *Recommended Practice for Determining the Peak Spatial-Average Specific Absorption Rate (SAR) in the Human Body from Wireless Communications Devices, 30 MHz–6 GHz: General Requirements for using the Finite Difference Time Domain (FDTD) Method for SAR Calculations,* IEEE 1528.1, Apr. 2006, draft standard,
28. Beard BB, Kainz W. Review and standardization of cell phone exposure calculations using the SAM phantom and anatomically correct head models. Biomed Eng Online. Oct 13.2004 3:34. [PubMed: 15482601]
29. ICNIRP (International Commission on Non-Ionizing Radiation Protection). Guidelines for limiting exposure to time-varying electric, magnetic and electromagnetic fields (Up to 300 GHz). Health Phys. 74:1998, 494–522.
30. *IEEE Standard for Safety Levels With Respect to Human Exposure to Radio Frequency Electromagnetic Fields, 3kHz to 300 GHz, Amendment 2: Specific Absorption Rate (SAR) Limits for the Pinna*, IEEE Standard C95.1b-2004, 2004.
31. *IEEE Recommended Practice for Measurements and Computations of Radio Frequency Electromagnetic Fields with Respect to Human Exposure to Such Fields, 100 kHz–300 GHz*, IEEE Standard C95.3-2002, 2002.
32. Anderson V. Comparisons of peak SAR levels in concentric sphere head models of children and adults for irradiation by a dipole at 900 MHz. Phys Med Biol. 2003; 48:3263–3275. [PubMed: 14620057]
33. Schönborn F, Burkhardt M, Kuster N. Differences in energy absorption between heads of adults and children in the near field of sources. Health Phys. Feb.1998 74:160–168. [PubMed: 9450585]

34. Kuster N, Balzano Q. Energy absorption mechanism by biological bodies in the near field of dipole antennas above 300 MHz. IEEE Trans Veh Technol. Feb; 1992 41(1):17–23.

35. Dielectric Properties of Body Tissue in the frequency range 10 Hz–100 GHz. Italian National Research Council, Institute for Applied Physics; Florence, Italy: [Online]. Available: http://niremf.ifac.cnr.it/tissprop/

36. Kainz W, Christ A, Kellom T, Seidman S, Nikoloski N, Beard B, Kuster N. The specific anthropomorphic mannequin (SAM) compared to 14 anatomical head models using a novel definition for the mobile phone positioning. Phys Med Biol. to be published.

Biographies

Brian B. Beard received the B.S. degree in electrical engineering from the U.S. Air Force Academy, Colorado Springs, CO, in 1973 and the M.S. and Ph.D. degrees from Vanderbilt University, Nashville, TN, in 1993 and 1995, respectively, both in biomedical engineering.

He is with the Center for Devices and Radiological Health, U.S. Food and Drug Administration, Rockville, MD. His current research interests include RF dosimetry and auditory prosthetics.

Wolfgang Kainz (M'02) worked for the Austrian Research Centers Seibersdorf (ARCS) and was the Associate Director of the Foundation for Research on Information Technologies in Society (IT'IS), Zurich, Switzerland. He is with the Center for Devices and Radiological Health, U.S. Food and Drug Administration, Rockville, MD.

Mr. Kainz is the Chairman of the IEEE/ICES, Technical Committee 34, Sub-Committee 2, which develops compliance techniques for wireless devices.

Teruo Onishi (M'00) received the B.S. degree in physics from the Tokyo University of Science, Tokyo, Japan, in 1987 and the Ph.D. degree in electrical engineering from Chiba University, Chiba, Japan, in 2005.

He is currently a senior research engineer at Wireless Laboratories, NTT DoCoMo Inc., Kanagawa, Japan.

Takahiro Iyama received the B.S. degree in electrical and electornic engineering and the M.S. degree in physical electronics from the Tokyo Institute of Technology, Tokyo, Japan, in 1996 and 1998, respectively.

He has been with NTT DoCoMo, Inc., Kanagawa, Japan, where he is engaged in research on EMC and bielectromagnetics.

Soichi Watanabe (S'93–M'96) received the Ph.D. degree from the Tokyo Metropolitan University, Hachioji city, Tokyo, Japan, in 1996, in electrical engineering.

He is leading the Biomedical EMC Group of the National Institute of Information and Communications Technology (NICT), Tokyo.

Osamu Fujiwara (M'84) received the B.E. degree from the Nagoya Institute of Technology, Nagoya, Japan, in 1971 in electronic engineering and the M.E. and D.E. degrees from the University, in 1973 and 1980, respectively, both in electrical engineering.

He is a Professor at the Nagoya Institute of Technology. His research interests include measurement and control of electromagnetic interference due to discharges, bioelectromagnetics, and other related EMC areas.

Jianqing Wang is a Professor of electrical and electronic engineering at the Nagoya Institute of Technology, Nagoya, Japan. His research interests include biomedical communications and electromagnetic compatibility.

Giorgi Bit-Babik (M'97) received the Ph.D. degree in radio physics and electronics from the Tbilisi State University (TSU), Tbilisi, Georgia, in 1998.

He was an Associate Professor at the TSU. In 2001, he joined the Motorola Corporate EME Research Laboratory, Fort Lauderdale, FL, where he is the Principal Staff Engineer. He is the holder of seven current and pending patents in antenna technology. His research interests include RF dosimetry and antenna research.

Antonio Faraone (M'97–SM'05) received the Ph.D. degree from the University of Rome *La Sapienza*, Rome, Italy, in 1997, in applied electromagnetics.

He is the Antenna R&D Manager at the Motorola Corporate EME Research Laboratory, Fort Lauderdale, FL. He holds eight patents in antenna technology. He is involved in EME related standards and RF dosimetry research.

Joe Wiart (M'96–A'01–SM'02) received the engineering degree from the École Nationale Supérieure des Telecommunication, Paris, France, in 1992 and the Ph.D. degree in physics from the École Nationale Supérieure des Télécommunications (ENST) and Pierre and Marie Curie University (Paris IV), Paris, in 1995.

He is with the France Télécom RD, Issy Moulineaux, France. His research interests include EMC, bioelectromagnetics, antenna measurements, computational electromagnetics, and signal processing.

Dr. Wiart is the Chairman of the CENELEC TC 211 working group in charge of mobile and base-station standards and the Chairman of the URSI French commission K.

Andreas Christ received the Dipl. Ing. degree from the Technical University of Darmstadt, Darmstadt, Germany, in 1996, in electrical engineering and the doctoral degree from the Swiss Federal Institute of Technology (ETH), Zurich, Switzerland, in 2003.

He is with the IT'IS Foundation, Zurich. His research interests include the use of numerical methods for the analysis of RF fields in the presence of biological tissues.

Niels Kuster (M'93) received the M.Sc. and Ph.D. degrees from the Swiss Federal Institute of Technology (ETH), Zurich, Switzerland, in electrical engineering in 1984 and 1992, respectively.

In 1993, he was a Professor at the Department of Electrical Engineering, ETH. In 1992, he was an Invited Professor with the Electromagnetics Laboratory, Motorola Inc., Fort Landerdale, FL, and in 1998 with the Metropolitan University of Tokyo, Tokyo, Japan. In 1999, he was appointed as the Director of the Foundation for Research on Information Technologies in Society, Zurich. His research interest is focused on the area of reliable on/in-body wireless communications and related topics.

Ae-Kyoung Lee received the B.S. and M.S. degrees from the Chungang University, Seoul, Korea, in 1990 and 1992, respectively, and the Ph.D. degree from the Chungnam National University, Daejeon, Korea, in 2003.

Since 1992, she is with the Electronics and Telecommunications Research Institute, Daejeon, where she has been engaged in research on numerical analysis and measurement of EMC and biological effects of electromagnetic fields.

Hugo Kroeze received the B.S. degree in electrical engineering in 1977 and the Ph.D. degree in biomedical engineering in 2002.

Since 1981, he is with the Biomedical Engineering Department, Utrecht University Hospital, working mainly on hyperthermia.

Martin Siegbahn received the M.Sc. degree from the Uppsala University, Uppsala, Sweden, in 1995, in engineering physics.

In 1995, he joined the Ericsson Research and the EMF Health and Safety Department. Since 2000, he has been a Senior Research Engineer with his main focus on RF exposure from wireless terminals.

Jafar Keshvari received the B.Sc. degree from the Middle East Technical University (METU), Ankara, Turkey, in 1989, in electrical and electronics engineering, and the M.Sc. degree from the Tampere University of Technology, Tampere, Finland, in biomedical engineering in 1994.

In 1999, he joined the Nokia Research Center, Helsinki, Finland, where he is involved in EMF health issues and computational dosimetry. His research interests in bioelectromagnetism includes modeling of head and eye to study EOG and ERG signals.

Houman Abrishamkar received the B.S. degree (*cum laude*) from the University of Ottawa, Ottawa, ON, Canada, and the M.A.Sc. degree from the University of Victoria, Victoria, BC, Canada, in 2003 and 2005, respectively, both in electrical engineering.

He is a Research Engineer with the Bioelectric Lab, University of Victoria.

Winfried Simon received the Dipl.-Ing. from the University of Duisburg, Duisburg, Germany, in 1997, in electrical engineering.

He is currently with IMST GmbH, Kamp-Lintfort, Germany, and is working in the department of Antennas and EM Modeling. He is the author or coauthor of more than 30 scientific publications. His research interests include passive component design and EM modeling.

Dirk Manteuffel received the Dipl.-Ing. and Dr.-Ing. degrees from the University of Duisburg-Essen, Duisburg, Germany, in 1998 and 2002, respectively, both in electrical engineering.

He is currently with IMST GmbH, Kamp-Lintfort, Germany. His research interests include terminal antennas, EM modeling, and UWB. He has published more than 40 scientific publications. He holds six patents.

Dr. Manteuffel received the Vodafone Innovations Award in 2004.

Neviana Nikoloski received the M.S. degree from the Sofia University “St. Kliment Ohridsky,” Sofia, Bulgaria, in 1996, in engineering physics. She is currently pursuing the Ph.D. degree at the Swiss Federal Institute of Technology (ETH), Zurich, Switzerland.

In 2000, she joined the Foundation for Research on Information Technologies in Society (IT’IS), Zurich.

Ms. Nikoloski received the first and second place BEMS Curtis Carl Johnson Memorial Awards in 2003 and 2002, respectively.

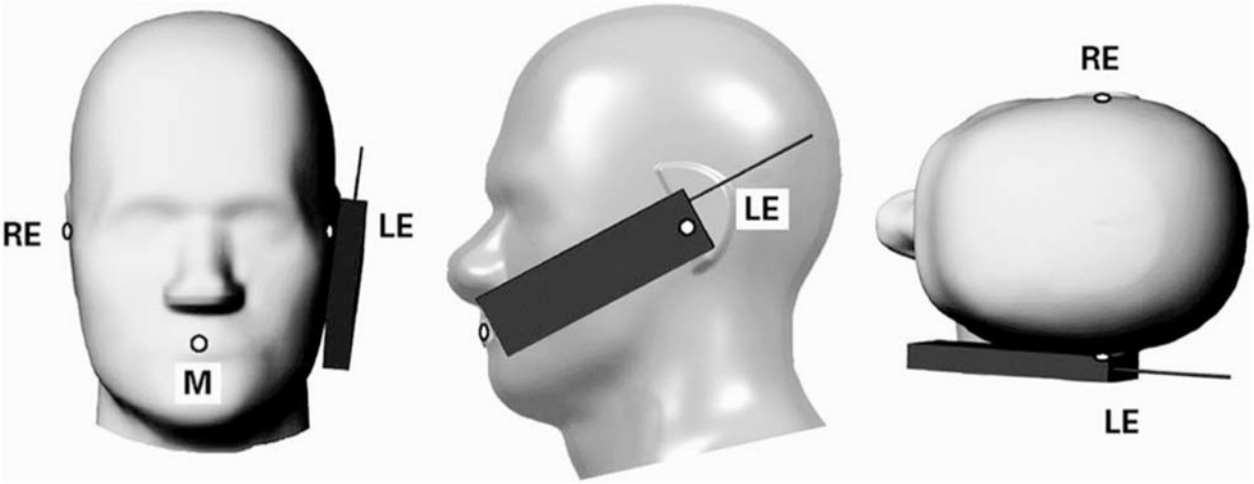

Fig. 1.

Specific Anthropomorphic Mannequin with cell phone in *Cheek* position on the left side. RE = Right Ear, LE = Left Ear, and M = Mouth.

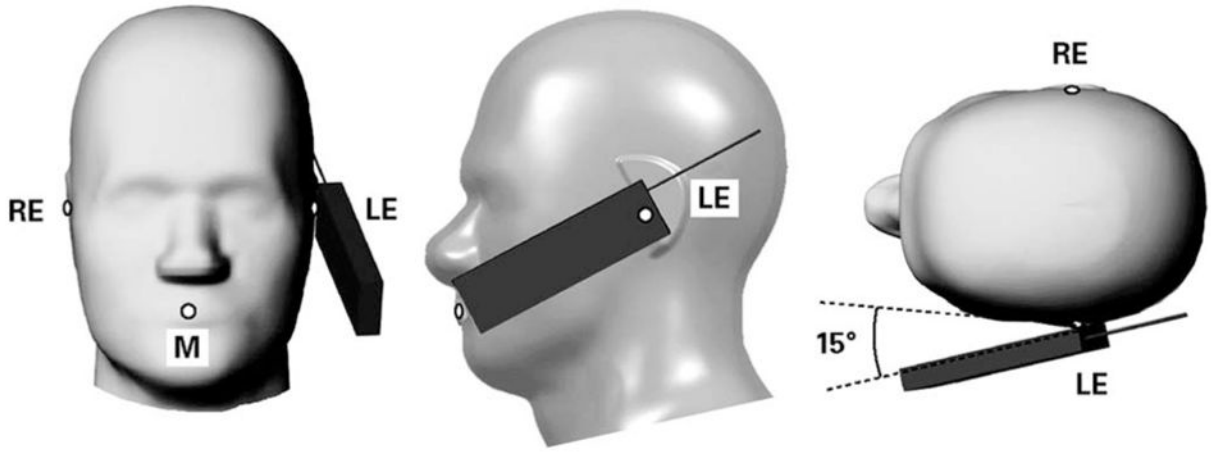

Fig. 2.

Specific Anthropomorphic Mannequin with cell phone in *Tilt* position on the left side. RE = Right Ear, LE = Left Ear, and M = Mouth.

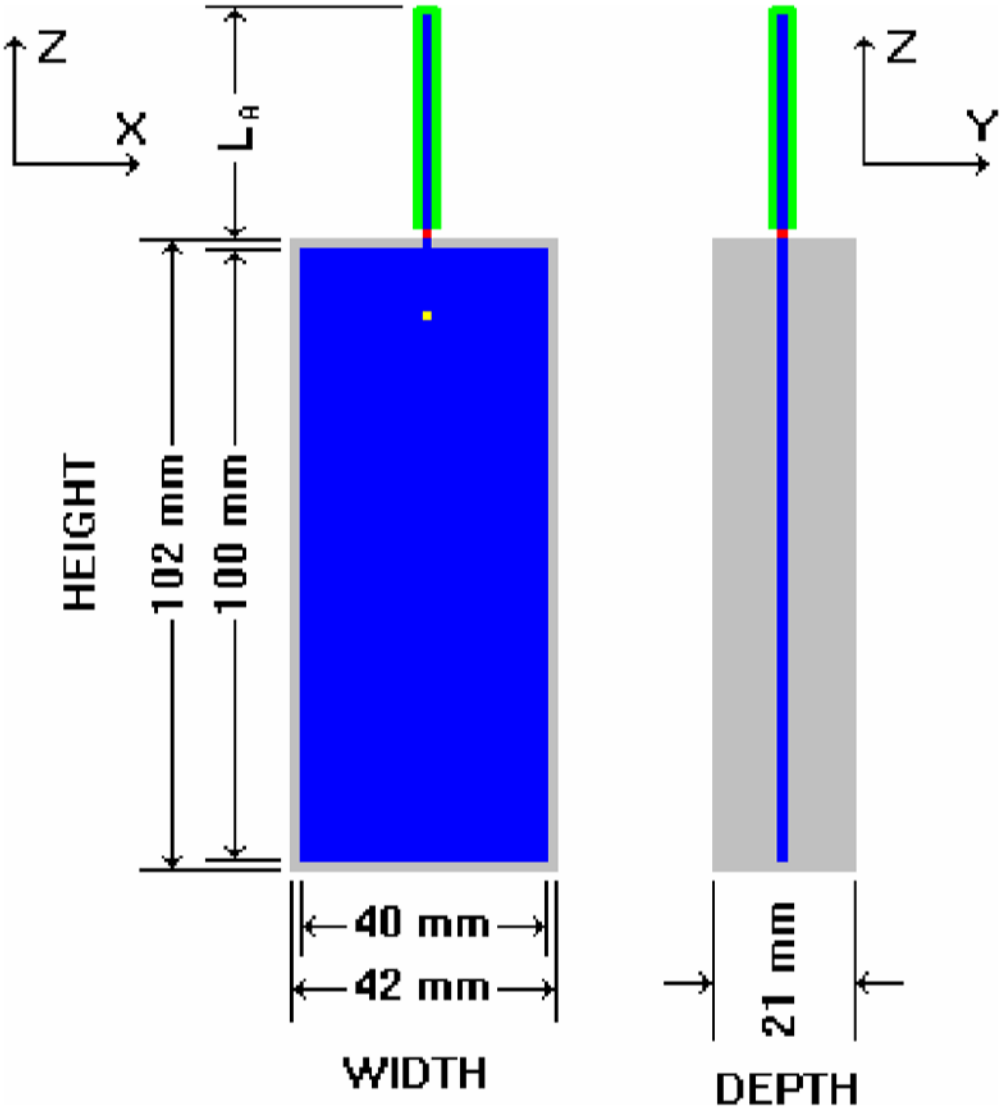

Fig. 3.

Generic cell phone designed for the intercomparison protocol. Blue = perfect electrical conductor, gray = plastic insulator, green = rubber insulator, and red = antenna feed-point voltage source. (Color version available online at http://ieeexplore.ieee.org.)

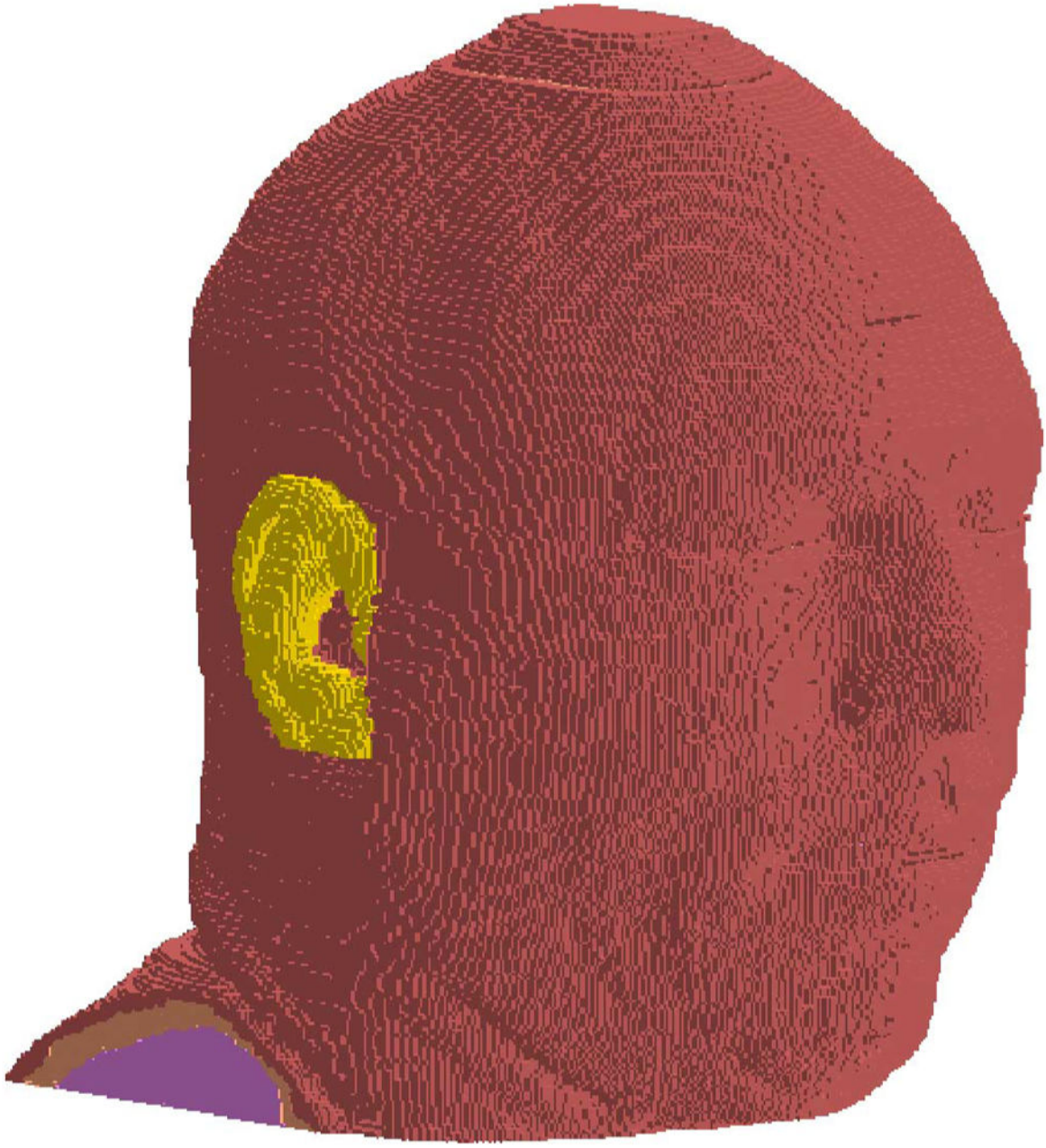

Fig. 4.

Visible Human head model used in the intercomparison protocol. The yellow voxels are the pinna. (Color version available online at http://ieeexplore.ieee.org.)

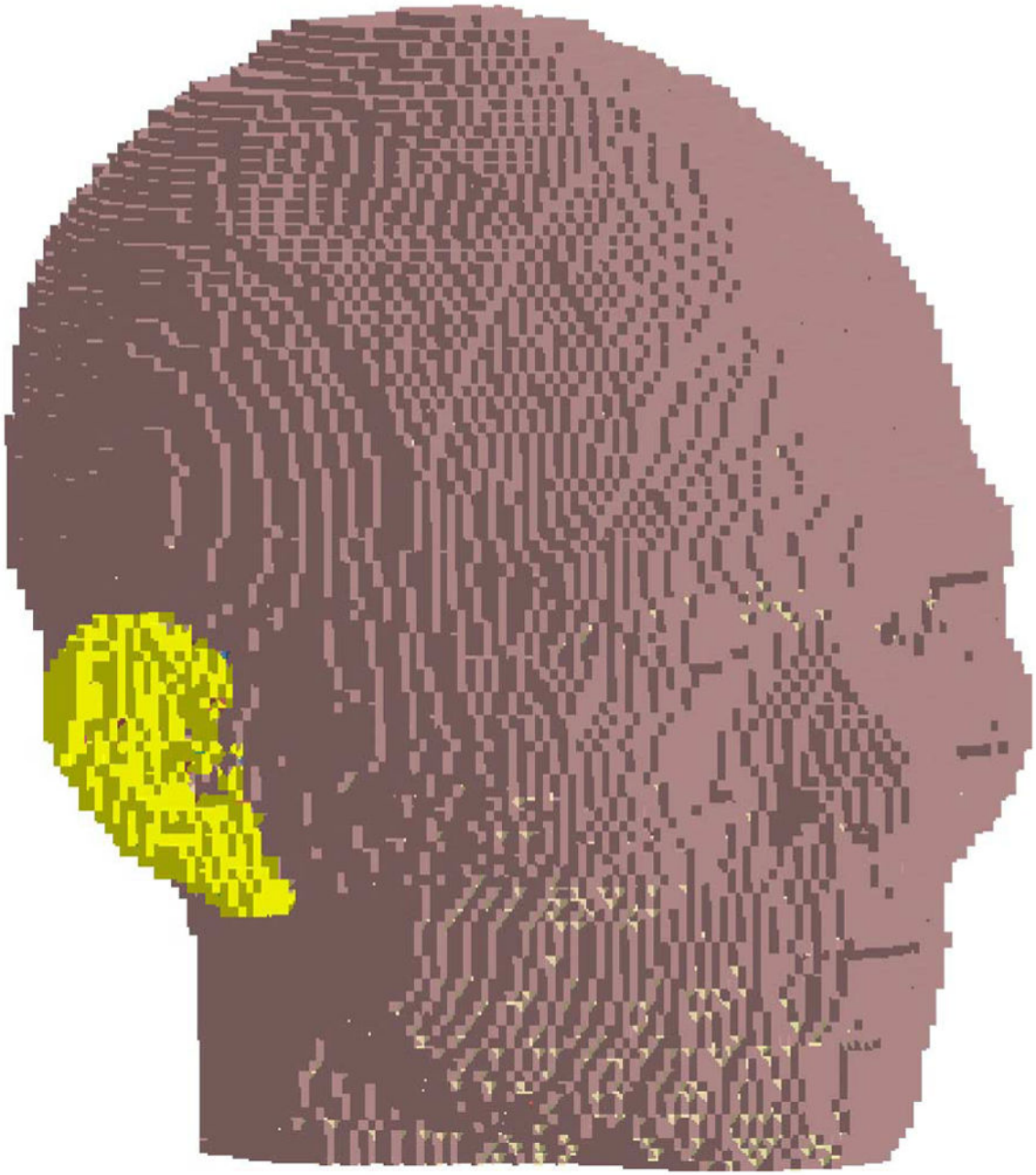

Fig. 5.

Seven-year-old Japanese male head model used in the intercomparison protocol. The yellow voxels are the pinna. (Color version available online at http://ieeexplore.ieee.org.)

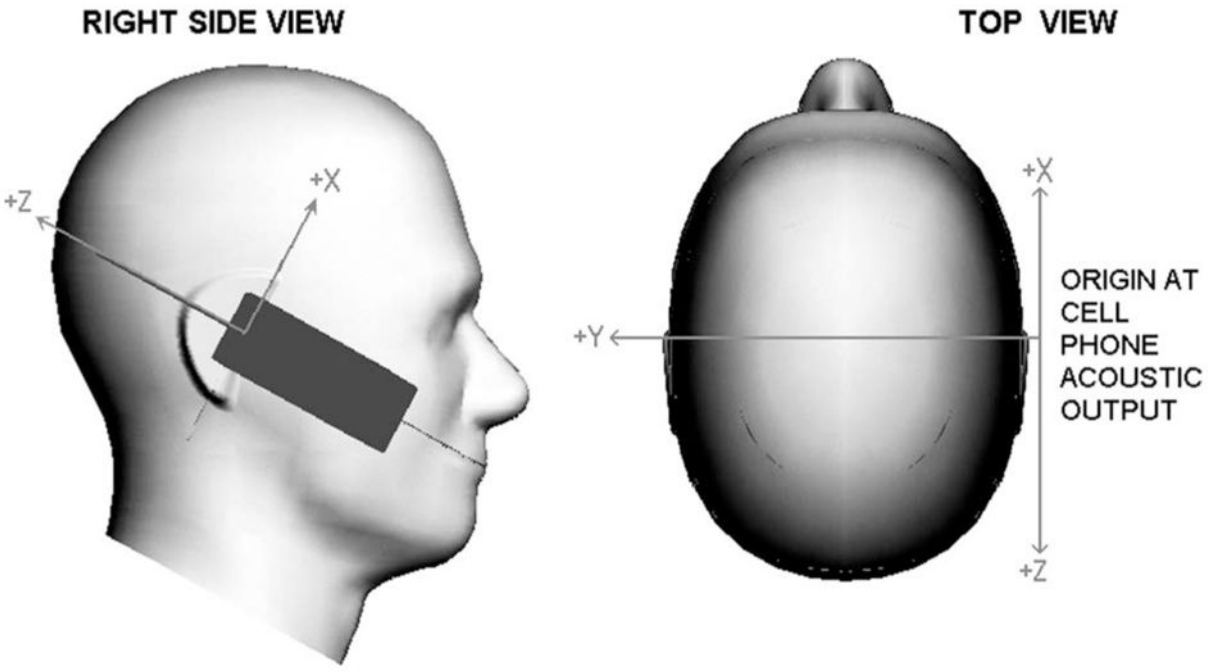

Fig. 6.

Left image shows the cell phone referenced coordinate system as seen from the right side of the specific anthropomorphic mannequin (SAM). The right image shows the coordinate system as seen from the top of the SAM. The SAM Ear Reference Points, left and right, are where the Y-axis intercepts the surface of the mannequin.

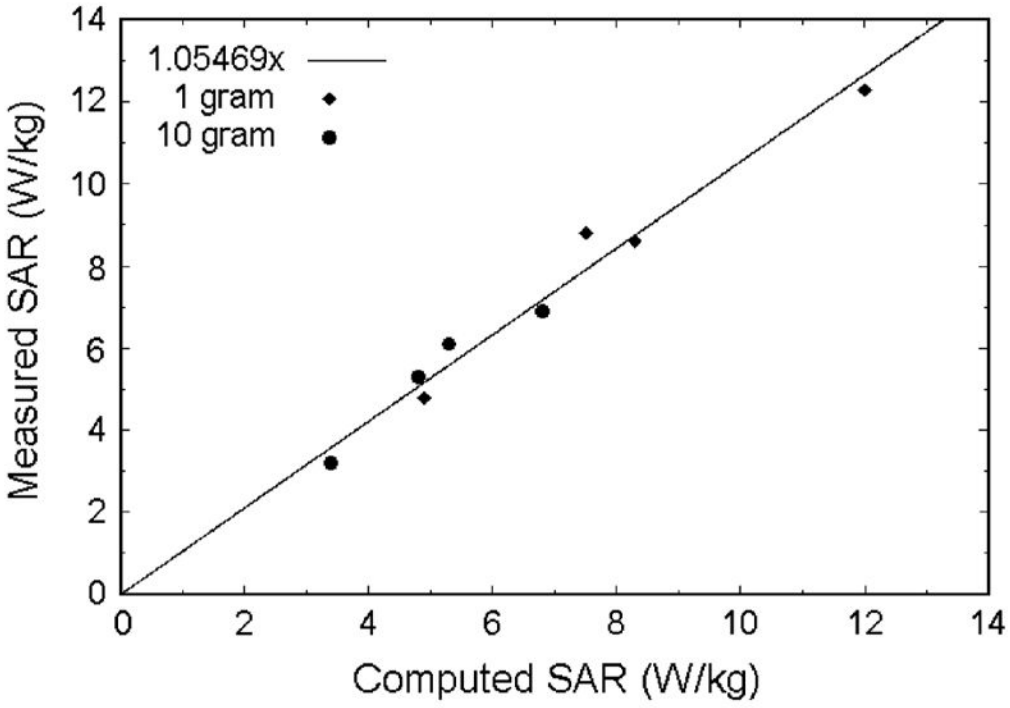

Fig. 7.

SAR measured with physical generic mobile phone and SAM versus SAR computed with simulated generic mobile phone and SAM. All SAR values are normalized to 1-W input power. The solid line is the least squares fit to the data.

TABLE I

Pooled SAR Statistics for All Models and Conditions for 835 MHz in the *CHEEK* Position

	Frequency - Position		835MHz - Cheek					
	Model		7-Yr		Adult		SAM	
	Normalization		1W	200mA	1W	200mA	1W	200mA
All Tissue	Peak 1g SAR W/kg	Mean	5.68	12.84	5.75	10.12	na	na
		Std Dev	1.28	2.21	0.73	2.04	na	na
		n	13	11	16	13	na	na
	Peak 10g SAR W/kg	Mean	2.87	6.47	3.92	6.89	na	na
		Std Dev	0.54	1.06	0.35	1.20	na	na
		n	13	11	16	13	na	na
Only Head Tissue	Peak 1g SAR W/kg	Mean	4.10	8.96	5.36	9.50	7.47	14.30
		Std Dev	0.35	1.19	0.47	1.66	0.40	1.26
		n	13	11	15	12	16	13
	Peak 10g SAR W/kg	Mean	2.33	5.11	3.72	6.57	5.26	10.08
		Std Dev	0.17	0.77	0.49	1.45	0.27	1.00
		n	13	11	15	12	16	13
Only Pinna Tissue	Peak 1g SAR W/kg	Mean	5.47	12.08	5.21	9.37	na	na
		Std Dev	1.30	2.60	0.67	1.90	na	na
		n	12	11	13	12	na	na
	Peak 10g SAR W/kg	Mean	2.90	6.37	3.33	5.74	na	na
		Std Dev	0.57	1.14	0.26	0.40	na	na
		n	10	9	11	10	na	na

TABLE II

Pooled SAR Statistics for All Models and Conditions for 835 MHz in the *TILT* Position

	Frequency - Position		835MHz - Tilt					
	Model		7-Yr		Adult		SAM	
	Normalization		1W	200mA	1W	200mA	1W	200mA
All Tissue	Peak 1g SAR W/kg	Mean	6.08	13.72	5.26	9.50	na	na
		Std Dev	1.59	2.92	1.06	2.18	na	na
		n	13	11	16	13	na	na
	Peak 10g SAR W/kg	Mean	2.90	6.71	3.13	5.63	na	na
		Std Dev	0.86	1.48	0.43	1.01	na	na
		n	13	11	16	13	na	na
Only Head Tissue	Peak 1g SAR W/kg	Mean	3.36	7.07	3.75	6.93	4.93	9.84
		Std Dev	0.86	1.46	0.58	1.80	0.64	0.98
		n	13	11	15	12	16	13
	Peak 10g SAR W/kg	Mean	1.68	3.61	2.51	4.58	3.39	6.75
		Std Dev	0.34	0.54	0.43	1.03	0.26	0.37
		n	13	11	15	12	16	13
Only Pinna Tissue	Peak 1g SAR W/kg	Mean	5.82	12.74	5.55	10.13	na	na
		Std Dev	1.56	3.16	1.31	3.02	na	na
		n	12	11	13	12	na	na
	Peak 10g SAR W/kg	Mean	2.87	6.32	3.30	5.95	na	na
		Std Dev	0.71	1.22	0.52	1.08	na	na
		n	10	9	11	10	na	na

TABLE III

Pooled SAR Statistics for All Models and Conditions for 1900 MHz in the *CHEEK* Position

	Frequency - Position		1900MHz - Cheek					
	Model		7-Yr		Adult		SAM	
	Normalization		1W	200mA	1W	200mA	1W	200mA
All Tissue	Peak 1g SAR W/kg	Mean	7.72	11.72	9.79	11.39	na	na
		Std Dev	2.38	2.64	3.41	1.55	na	na
		n	13	11	16	13	na	na
	Peak 10g SAR W/kg	Mean	3.96	6.13	5.12	6.02	na	na
		Std Dev	0.89	1.12	1.78	0.67	na	na
		n	13	11	16	13	na	na
Only Head Tissue	Peak 1g SAR W/kg	Mean	5.23	7.55	5.93	7.42	8.28	10.84
		Std Dev	1.68	1.36	1.51	2.26	1.58	1.17
		n	13	11	15	12	16	13
	Peak 10g SAR W/kg	Mean	2.91	4.20	3.17	3.86	4.79	6.21
		Std Dev	0.85	0.64	0.87	1.39	0.73	0.56
		n	13	11	15	12	16	13
Only Pinna Tissue	Peak 1g SAR W/kg	Mean	7.96	11.68	9.09	11.47	na	na
		Std Dev	2.31	2.54	1.86	1.95	na	na
		n	12	11	13	12	na	na
	Peak 10g SAR W/kg	Mean	4.63	6.69	5.99	7.68	na	na
		Std Dev	1.04	0.84	1.03	1.05	na	na
		n	10	9	11	10	na	na

TABLE IV

Pooled SAR Statistics for All Models and Conditions for 1900 MHz in the *TILT* Position

	Frequency - Position		1900MHz - Tilt					
	Model		7-Yr		Adult		SAM	
	Normalization		1W	200mA	1W	200mA	1W	200mA
All Tissue	Peak 1g SAR W/kg	Mean	9.81	17.87	15.76	22.75	na	na
		Std Dev	6.75	10.45	4.58	8.95	na	na
		n	12	11	15	13	na	na
	Peak 10g SAR W/kg	Mean	4.71	8.76	8.14	11.69	na	na
		Std Dev	2.04	3.35	2.24	4.58	na	na
		n	12	11	15	13	na	na
Only Head Tissue	Peak 1g SAR W/kg	Mean	4.19	7.46	7.91	11.53	11.97	19.17
		Std Dev	0.80	1.14	1.57	3.90	3.10	4.33
		n	12	11	14	12	15	13
	Peak 10g SAR W/kg	Mean	1.85	3.30	3.53	5.23	6.78	10.77
		Std Dev	0.52	0.78	0.72	2.02	1.37	1.85
		n	12	11	14	12	15	13
Only Pinna Tissue	Peak 1g SAR W/kg	Mean	9.87	17.12	15.92	23.93	na	na
		Std Dev	7.03	10.58	5.77	12.41	na	na
		n	11	11	12	12	na	na
	Peak 10g SAR W/kg	Mean	5.38	9.36	9.78	14.72	na	na
		Std Dev	2.76	4.03	2.65	6.12	na	na
		n	9	9	10	10	na	na

TABLE V

SAR Measured With Physical Generic Mobile Phone and SAM, and SAR Computed With Simulated Generic Mobile Phone and SAM. All SAR Values Are Normalized to 1 W Input Power

	Computed Averages		Measured	
	1-gram	**10-gram**	**1-gram**	**10-gram**
835MHz Cheek	7.5	5.3	8.8	6.1
835MHz Tilt	4.9	3.4	4.8	3.2
1900MHz Cheek	8.3	4.8	8.6	5.3
1900MHz Tilt	12.0	6.8	12.3	6.9

TABLE VI

Statistics for Reported Distance (mm) Between the Generic Mobile Phone Feed Point and the Nearest Tissue Voxel for *CHEEK* Apposition

	Model		
	7-Yr	**Adult**	**SAM**
Min	8.60	10.00	11.00
Mean	11.53	13.08	15.51
Max	14.90	18.49	19.10
Std. Dev.	1.77	2.02	3.09
n	11	12	12

Feedpoint to tissue distance (nm) for ciieek position.

TABLE VII

Statistics for Reported Distance (mm) Between the Generic Mobile Phone Feed Point and the Nearest Tissue Voxel for *TILT* Position

	Model		
	7-Yr	**Adult**	**SAM**
Min	8.25	10.00	10.00
Mean	11.69	11.67	13.46
Max	14.00	13.42	18.10
Std. Dev.	1.77	1.01	3.34
n	10	12	11

TABLE VIII

Mean SAR and Standard Deviation for Head Tissue for All Models. All Values Are Expressed as a Percentage of (Normalized By) the Mean SAR From SAM for the Same Conditions

	Tissue in SAR Volume		Only Head Tissue					
	Model		7-Yr		Adult		SAM	
	Normalization		1W	200mA	1W	200mA	1W	200mA
835MHz Cheek	Peak 1g SAR	Mean	54.9%	62.7%	71.7%	66.5%	100.0%	100.0%
		Std Dev	4.7%	8.3%	6.3%	11.6%	5.4%	8.8%
	Peak 10g SAR	Mean	44.2%	50.7%	70.7%	65.2%	100.0%	100.0%
		Std Dev	3.3%	7.7%	9.3%	14.4%	5.2%	9.9%
835MHz Tilt	Peak 1g SAR	Mean	68.1%	71.9%	76.0%	70.4%	100.0%	100.0%
		Std Dev	17.4%	14.9%	11.8%	18.3%	12.9%	10.0%
	Peak 10g SAR	Mean	49.5%	53.6%	73.9%	67.9%	100.0%	100.0%
		Std Dev	10.1%	8.1%	12.7%	15.3%	7.6%	5.5%
1900MHz Cheek	Peak 1g SAR	Mean	63.1%	69.6%	71.6%	68.4%	100.0%	100.0%
		Std Dev	20.3%	12.6%	18.2%	20.8%	19.1%	10.8%
	Peak 10g SAR	Mean	60.7%	67.6%	66.1%	62.2%	100.0%	100.0%
		Std Dev	17.7%	10.4%	18.2%	22.4%	15.2%	9.1%
1900MHz Tilt	Peak 1g SAR	Mean	35.0%	38.9%	66.1%	60.2%	100.0%	100.0%
		Std Dev	6.7%	5.9%	13.1%	20.3%	25.9%	22.6%
	Peak 10g SAR	Mean	27.3%	30.7%	52.0%	48.6%	100.0%	100.0%
		Std Dev	7.6%	7.2%	10.6%	18.7%	20.2%	17.2%

TABLE IX

Mean SAR and Standard Deviation for Only Pinna Tissue in the Anatomic Models. All Values Are Expressed as a Percentage of (Normalized By) the Mean Head Only SAR From SAM for the Same Conditions

	Tissue in SAR Volume		Only Pinna Tissue				Only Head Tissue	
	Model		7-Yr		Adult		SAM	
	Normalization		1W	200mA	1W	200mA	1W	200mA
835MHz Cheek	Peak 1g SAR	Mean	73.2%	84.5%	69.7%	65.6%	100.0%	100.0%
		Std Dev	17.5%	18.2%	8.9%	13.3%	5.4%	8.8%
	Peak 10g SAR	Mean	55.2%	63.2%	63.3%	56.9%	100.0%	100.0%
		Std Dev	10.8%	11.3%	5.0%	3.9%	5.2%	9.9%
835MHz Tilt	Peak 1g SAR	Mean	118.0%	129.5%	112.5%	102.9%	100.0%	100.0%
		Std Dev	31.6%	32.1%	26.6%	30.7%	12.9%	10.0%
	Peak 10g SAR	Mean	84.4%	93.7%	97.2%	88.3%	100.0%	100.0%
		Std Dev	20.8%	18.1%	15.3%	15.9%	7.6%	5.5%
1900MHz Cheek	Peak 1g SAR	Mean	96.1%	107.8%	109.7%	105.8%	100.0%	100.0%
		Std Dev	27.9%	23.4%	22.5%	18.0%	19.1%	10.8%
	Peak 10g SAR	Mean	96.7%	107.8%	125.1%	123.7%	100.0%	100.0%
		Std Dev	21.6%	13.6%	21.5%	17.0%	15.2%	9.1%
1900MHz Tilt	Peak 1g SAR	Mean	82.5%	89.3%	133.0%	124.8%	100.0%	100.0%
		Std Dev	58.8%	55.2%	48.2%	64.7%	25.9%	22.6%
	Peak 10g SAR	Mean	79.3%	86.9%	144.3%	136.6%	100.0%	100.0%
		Std Dev	40.8%	37.4%	39.1%	56.8%	20.2%	17.2%

IEEE Trans Electromagn Compat. Author manuscript; available in PMC 2018 March 05.